Nuclear Inst. and Methods in Physics Research, A 1047 (2023) 167808

Contents lists available at ScienceDirect

Nuclear Inst. and Methods in Physics Research, A

journal homepage: www.elsevier.com/locate/nima

Design and characteristics of a novel single-plane Compton gamma camera based on GAGG scintillators readout by SiPMs

Om Prakash Dash *, Tomislav Bokulić, Damir Bosnar, Petar Žugec, Mihael Makek

Department of Physics, Faculty of Science, University of Zagreb, Bijenička c. 32, 10000, Zagreb, Croatia

ARTICLE INFO

Keywords:
Compton camera
Compton imaging
GAGG
SiPM

ABSTRACT

We designed a novel, compact, single-plane Compton gamma camera based on GAGG:Ce scintillators read out by silicon photomultipliers. The Compton gamma camera comprises the scatterer and the absorber layers consisting of 8x8 arrays of 3 mm × 3 mm × 3 mm GAGG:Ce pixels. The individual pixels in the scatterer layer are optically coupled to the corresponding pixels in the absorber by the matching 3 mm × 3 mm × 20 mm plexiglass lightguides, and hence both the scatterer and the absorber pixel in one column are readout by the same SiPM. We present the first results of the measured characteristics of the detector. The average energy resolution at 662 keV of the front and the back GAGG:Ce layer is found to be 8.9% ± 1.9% and 10.8% ± 1.6%, respectively. The Compton events are reconstructed based on kinematic conditions and detector geometry and the first image of a 662 keV gamma source is reconstructed using a simple back projection algorithm.

1. Introduction

Compton gamma camera (CGC) is a gamma-ray detector which, unlike the gamma cameras with mechanical collimation, determines the source position based on the kinematics of Compton scattering. The evolution of CGCs started with semiconductor detectors, which provide excellent spatial resolution [1,2], later shifted to scintillator detectors, initially with photo-multiplier tubes and more recently with Silicon photomultipliers (SiPMs) [3,4]. Scintillator based CGCs have lower, yet still acceptable, energy resolutions compared to the semiconductor ones, but higher efficiencies and lower cost. Most CGCs comprise two separate detector planes, the scatterer and the absorber, with recent attempts to make a single plane CGC to enhance compactness and reduce costs [5].

We designed and assembled a single-plane Compton gamma camera based on a novel concept with pixelated scintillators coupled with light guides read out on only one side by SiPMs.

2. Materials and methods

The detector concept is based on the scatterer (front) layer comprising scintillation pixels, connected by plexiglass lightguides to scintillators in the absorber (back) layer, which is coupled to SiPMs.

Geant4 simulations were performed to estimate the achievable angular resolution and intrinsic efficiency of detector configurations for lightguide lengths of 10 mm, 20 mm and 30 mm. We simulated a point source of 662 keV gammas at 10 cm from the detector and realistic detector resolution and geometry were implemented. We obtained the intrinsic efficiencies of 0.26, 0.11, 0.05 and the angular resolutions of 13.3°, 10.5°, 9.6°, respectively. The angular resolution measure was obtained from the difference of the known and the reconstructed source position, while the intrinsic efficiency was determined as the ratio of the incoming to detected gammas. The lightguide length of 20 mm is chosen for the final design as the best tradeoff between the efficiency and angular resolution.

The scatter layer comprises an 8 × 8 array of 3 mm × 3 mm × 3 mm polished GAGG:Ce scintillators with a 3.2 mm pitch. It is coupled to a layer of polished plexiglass light guides with 3 mm × 3 mm × 20 mm using optical cement (EJ-500, Eljen technology) coupled on the other side to matching GAGG:Ce pixel array in the absorption (back) layer. The latter is coupled to a matching 8 × 8 SiPMs (Hamamatsu, S13361-3050AE08). The GAGG scintillator is chosen for its superb energy resolution [6], an important factor in the performance of the CGC. In this concept, both the scatterer and the absorber pixels in one column are read out by the same SiPM, which keeps the number of readout channels at minimum. We first optically glued each detector column then assembled row by row using enhanced specular reflector foils (0.65 μm, 3M) as reflectors (Fig. 1). The SiPM was read out using TOFPET2 [7] and the environmental temperature was kept between 18–20 °C.

* Corresponding author.
E-mail address: ompd@phy.hr (O.P. Dash).

https://doi.org/10.1016/j.nima.2022.167808
Received 28 July 2022; Received in revised form 4 November 2022; Accepted 5 November 2022
Available online 15 November 2022

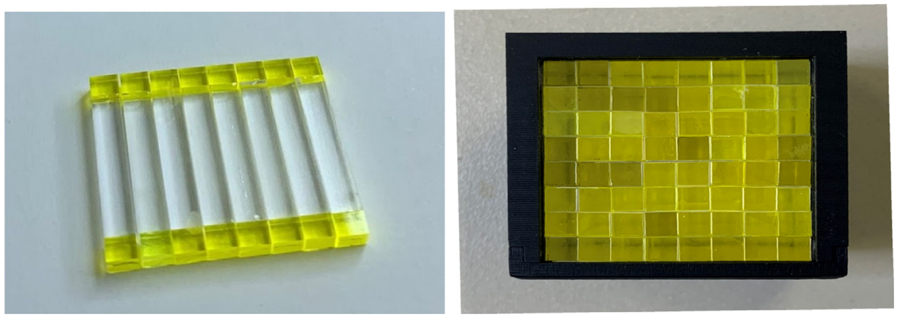

Fig. 1. A row of individual crystals (left), final assembly after inserting all 8 rows and reflector foils (right).

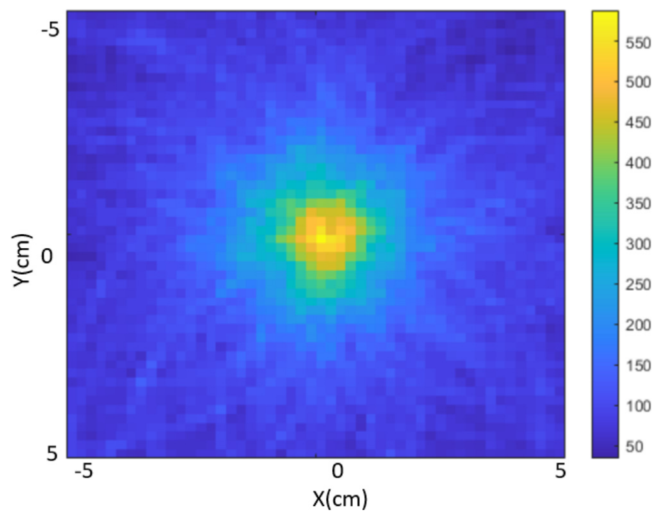

Fig. 2. Reconstructed image of the source.

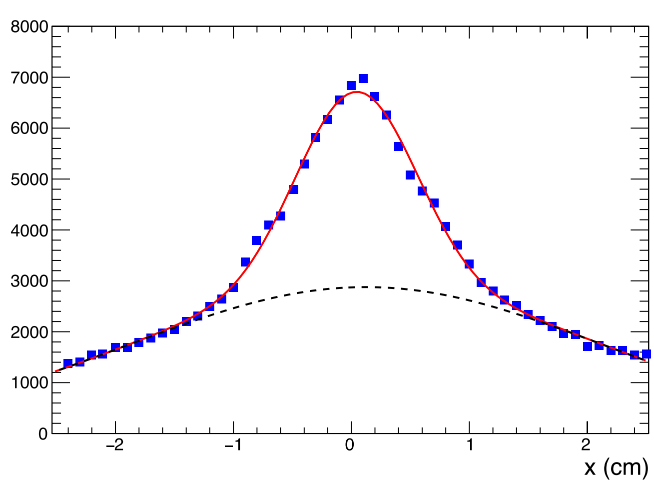

Fig. 3. Projection of the reconstructed image on x-axis fit with a Gaussian (red) on top of Gaussian background (black-dashed).

3. Result and discussion

We characterized the energy resolution of the front and the back detector layer individually, by irradiating the respective layers with the collimated source on the side. The average energy resolution at 662 keV of the front and the back GAGG:Ce layer is found to be 8.9 ± 1.9% and 10.8 ± 1.6% respectively, the uncertainty reflects variations within the module. We observed the front layer showing up to 20% higher signals, which we assigned to the fact that the front pixels have 5 reflective sides, while the back ones have only 4. The ratios of the 662 keV peak positions with the source collimated at the front/back layer, are used as correction factors once the front and the back pixels are identified.

The imaging capability was checked by placing a ^{137}Cs source (diam. ≈ 3 mm) 50 mm in front of the module. We reconstructed the Compton events requiring: (a) exactly two SiPM pixels fire with $E_{px} >$ 100 keV, (b) their energy sum corresponds to the full energy deposition (in this case 662 keV), (c) the energy of one of the pixels must be in the range 100–150 keV and (d) the transaxial distance between the pixel centres, $d = \sqrt{(x_1 - x_2)^2 + (y_1 - y_2)^2}$, in range 8 mm $< d <$ 20 mm. The low energy threshold of 100 keV was set to discriminate the noise, while the upper limit of 150 keV was applied to select the forward scattering events since the minimum energy deposit by the Compton backscattering is 184 keV. Thus conditions (a)–(c) kinematically limit the Compton scattering angles $30° \lesssim \theta_{\text{Compt}} \lesssim 42°$ and ensure that the pixel with the lower energy is located in the front layer. The condition (d) additionally filters the events corresponding to scattering angle range $30° \lesssim \theta_{\text{Compt}} \lesssim 42°$ as determined by the transaxial distance, d. The image of the source reconstructed using a simple back-projection algorithm is in Fig. 2 and the image projection shows a clear Gaussian peak with $\sigma = 5.1 \pm 0.2$ mm (Fig. 3) on top of Gaussian background.

4. Summary and outlook

We designed, assembled and tested a novel single-plane Compton gamma camera. We expect to improve its imaging performance by optimizing the analysis procedure and by using iterative reconstruction strategy on high statistics data samples. If the concept proves successful, a dedicated electronics will be developed for a transportable detector. This simple device may be a significant step in the realization of a compact, cost-effective and transportable CGC, with a realistic potential for scaling-up to application-specific larger systems.

Declaration of competing interest

The authors declare that they have no known competing financial interests or personal relationships that could have appeared to influence the work reported in this paper.

Acknowledgements

This work was supported in by the Croatian Science Foundation under project 8570 and by "Research Cooperability" Program of the Croatian Science Foundation funded by the European Union from the European Social Fund under the Operational Programme Efficient Human Resources 2014–2020, Grant number PZS-2019-02-5829.

References

[1] L. Kaufman, et al., IEEE Trans. Nucl. Sci. 27 (1980) 1073–1079.
[2] S. Boggs, et al., New Astron. Rev. 48 (2004) 251–255.
[3] G. Llosá, et al., NIM A 648 (2011) S96–S99.
[4] S. Jiang, et al., J. Instr. 16 (2021) P01027.
[5] J. Kataoka, et al., NIM A 732 (2013) 403–407.
[6] M. Makek, et al., Crystals 10 (12) (2020) 1073.
[7] A. Di Francesco, et al., J. Instr. 11 (2016) C03042.